

Journal of Chemical, Biological and Physical Sciences

An International Peer Review E-3 Journal of Sciences

Available online at www.jcbpsc.org

Section C: Physical Sciences



CODEN (USA): JCBPAT

Research Article

Effect of Substituents on the Photoluminescence Performance of Ir(III)Complexes: Synthesis and Photo Physical Properties

H.K. Dahule¹ and S.J.Dhoble²

¹Department of Physics Shivaji Science College, Nagpur-440012, India

²Department of Physics, RTM Nagpur University, Nagpur 440033, India

Received: 27 June 2012; Revised: 25 July 2012; Accepted: 30 July 2012

ABSTRACT

A series of substituted 2,4 diphenyl quinoline ligands namely (Cl-DPQ), (OMe –DPQ), and M-DPQ) have synthesized. These compounds readily undergo cyclometalation with iridium trichloride and form iridium (III) dopants of the substituted 2,4 diphenyl quinoline ligands. Synthesized compounds emit red color in solid as well as in solution phase. The peak emission wavelength of the dopants (λ_{max} = 610-650 nm) can be tuned depending upon the electronic properties of the methoxy, chloronine and methyl substituents as well as their positions in the 2,4 diphenyl quinoline ring. These synthesized iridium complexes were characterized by ¹HNMR, DTA/TGA, XRD, and FTIR . The molecular structure of M-DPQ, OMe-DPQ, Cl-DPQ Ir(M-DPQ)₂(acac) , Ir(OMe-DPQ)₂(acac) and Ir(Cl-DPQ)₂(acac) is confirmed by the FTIR spectra. The photo physical properties were studied by UV-vis absorption and photoluminescence. The synthesized quinoline-based iridium complexes are promising candidates for efficient red emitters.

Keywords: Phosphorescent, cyclometalation, organometallic, spectrofluorometer

INTRODUCTION

Heavy-metal complexes result in high efficient electro phosphorescence in organic light-emitting devices (OLEDs) because both singlet and triplet excitons can be harvested for light emission¹⁻³. The design and synthesis of phosphorescent emitting materials containing heavy-metal complexes are particularly important in achieving high-efficiency OLEDs.

In most OLEDs, triplet states constitute 75% of electro generated excited states. These triplet states are generally non-emissive due to their long lifetime (commonly from milliseconds to minutes) as well as their spin-forbidden nature for radioactive relaxation to the ground states. Consequently, the maximum internal quantum efficiency of OLEDs is normally limited to 25%. To remove such constraint, efforts have been directed in using transition metal complexes, particularly 4d and 5d metals³⁻⁵. The strong spin-orbit coupling caused by heavy metal ions in these complexes results in efficient intersystem crossing from the singlet to the triplet excited state. Mixing of the singlet and triplet excited states not only removes the spin-forbidden nature of the radiative relaxation of the triplet state but also significantly shortens the triplet state lifetime. Triplet-triplet annihilation is more effectively suppressed because of the shorter lifetime of the triplet excited state. Therefore, higher phosphorescence efficiencies can be achieved. Numerous organometallic d⁶, d⁸ and d¹⁰ complexes are luminescent in solution or solid state⁶⁻²³. Among these Os (II)¹³, Cu(I)¹⁴, cyclometalated Ir(III)¹⁵⁻²⁰ and Pt(II) complexes²¹⁻²⁴ have been fabricated into light-emitting devices. Cyclometalated iridium (III) complexes receive the most extensive study partly due to their ease of preparation from iridium precursors with the corresponding imines which are capable of undergoing cyclometalation³. Most of the iridium complexes used in these studies consists of cyclometalated 2, 4 diphenyl quinoline derivatives as ligands. Synthesis²⁵ and photo physical properties of some substituted 2, 4 diphenyl quinoline based Ir(III) complexes were also reported^{19,26-28}. Recently, good organic materials developed and characterized it's optical properties are important for development for lighting materials²⁹⁻³⁰.

In this paper, we report the synthesis, and photo physical properties of the Ir(OMe-DPQ)₂(acac), Ir(CL-DPQ)₂(acac) and Ir(M-DPQ)₂(acac) iridium complexes.

2. EXPERIMENTAL

2.1. Materials: All reagents and solvents were used as received without further purification. All reactions were performed under argon atmosphere.

2.1.1. General procedure for synthesis of quinoline ligands: The quinoline-derived ligands 2-(4 Chloro phenyl)-4-phenyl quinoline (Cl-DPQ), 2-(4 methyl phenyl)-4-phenyl quinoline (M-DPQ) and 2-(4 methoxy phenyl)-4-phenyl quinoline (OMe-DPQ) were synthesized conveniently according to Scheme 1 from the condensation of 2-aminobenzophenone and corresponding (4-chloro, P-Methyl, 4-methoxy) acetophenone using the acid-catalyzed Friedlander reaction³¹.

2.1.1.1. 2-(4 Chloro phenyl)-4-phenyl quinoline (Cl-DPQ): Yield: 72%. ¹H NMR(300 MHz, CDCl₃): δ 7.47–7.56 (m, 9H), 7.74 (t, *J* = 7.6 Hz, 1H), 7.83 (s, 1H), 7.91 (d, *J* = 8.4 Hz, 1H), 8.20 (d, *J* = 7.4 Hz, 2H), 8.26 (d, *J* = 8.4 Hz, 1H).

An elemental analysis of the polymeric material chlorine substituted 2, 4- diphenyl quinoline (Cl-DPQ) measured using Thermo Finnigan, Flash 1112 Series EA model is Anal. Calcd. For C₂₁H₁₆ClN=317 found 317.5 C, 79.70; H, 5.04; N, 4.21. Cl, 11.05 % Found: C, 79.68; H, 5.06; N, 4.19; Cl, 11.17 %.

2.1.1.2. 2-(4 methyl phenyl)-4-phenyl quinoline (M-DPQ) : Yield: 71%. ¹H NMR (300 MHz, CDCl₃): δ 3.78 (s, 3H), 7.02 (d, *J* = 8.2 Hz, 2H), 7.42 (td, *J* = 7.1, 1.3 Hz, 1H), 7.51–7.59 (m, 5H), 7.73 (td, *J* = 7.2, 1.3 Hz, 1H), 7.83 (s, 1H), 7.94 (d, *J* = 8.4 Hz, 1H), 8.20 (d, *J* = 8.5 Hz, 2H), 8.27 (d, *J* = 8.4 Hz, 1H). CHN Calcd for C₂₂H₁₇N 295.226, found 295.242. Anal Calcd for C₂₂H₁₇N C=89.46, H=5.75, N=4.72, Found C=89.50%, H=5.76%, N=4.74%.

2.1.1.3. 2-(4-Methoxy-phenyl)-4-phenyl-quinoline(OMe-DPQ): Yield: 73%. ¹H NMR (300 MHz, CDCl₃): δ 3.92 (s, 3H), 7.08 (d, *J* = 8.6 Hz, 2H), 7.47 (td, *J* = 7.6, 1.2 Hz, 1H), 7.54–7.59 (m, 5H), 7.73 (td, *J* = 7.6, 1.2 Hz, 1H), 7.78 (s, 1H), 7.87 (d, *J* = 8.4 Hz, 1H), 8.20 (d, *J* = 8.6 Hz, 2H), 8.23 (d, *J* = 8.5

Hz, 1H). CHN Calcd for C₂₂H₁₇NO 311.225, found 311.242. Anal Calcd for C₂₂H₁₇NO C=84.46, H=5.68, N=4.7, O=5.13 Found C=84.64, H=5.48, N=4.6, O=5.14.

2.1.2. General procedure for synthesis of Ir(III) complexes: Cyclometalated Ir(III)-chloro-bridged dimers were synthesized according to the Nonoyama method³². The mixture of IrCl₃·nH₂O (1 equiv.) and the quinoline ligand (2.5 equiv.) in 2-methoxyethanol/water (v/v: 3/1) was refluxed. The precipitate was collected by filtration and washed with water and ethanol. After dried, the crude product was directly used for next step without further purification. In the synthesis of final product, the mixture of the chloro-bridged dimer (1.0 mmol), acetyl acetone (2.5 mmol), and Na₂CO₃ (1.06 g, 10.0 mmol) in 2-ethoxyethanol (15 ml) had been refluxed in an inert atmosphere for 12-14 h before cooled to room temperature. A red precipitate was collected and washed with water and ethanol to afford pure product with the yield in the range of 28–75%.

2.1.2.1. Bis(2- (4 Chloro phenyl)- 4phenyl quinoline)iridium(acetylacetonate) Ir (Cl-DPQ)₂ (acac): . Yield 79.24 %. ¹H-NMR(300MHz CDCl₃) 6.6 -8.0 (m,26H) 4.6-8 (S,1H) 2.7 (S,6H) 1.5 (S,6H) CHN Calcd for C₄₇ H₃₇ O₂ N₂ Cl Ir 888.43, found 888 Anal Calcd for C₄₇ H₃₇ O₂ N₂ Cl Ir C,64.33, H ,4.26, N ,3.06,Cl,3.87. Found C,64.02, H,4.32, N,3.08, Cl,3.56.

2.1.2.2. Bis(2- (4 methyl phenyl) 4-phenyl quinoline)iridium(acetylacetonate) Ir (M-DPQ)₂ (acac): Yield 78% ¹H - NMR(300MHz CDCl₃) 6.7 -8.0 (m,26H) 4.7-8 (S,1H) 2.5 (S,6H) 1.5 (S,6H) CHN Calcd for C₄₉ H₃₉ O₂ N₂ Cl Ir 914, found 914 Anal Calcd for C₄₉ H₃₉ O₂ N₂ Cl Ir C=64.33, H =4.26, N =3.06, Found C=64.01, H=4.31, N=3.09,

2.1.2.3. Bis(2-(4-Methoxy-phenyl)-4-phenyl-quinoline)iridium(acetylacetonate): Ir(OMe-DPQ)₂(acac) : Yield: 48%. Anal. Calcd for C₄₉H₃₉N₂O₄Ir: C, 64.53; H, 4.31; N, 3.07. Found: C, 64.18; H, 4.26; N, 2.99. ¹H-NMR(300 MHz, CDCl₃):δ 1.56 (s, 6H), 3.43 (s, 6H), 4.73 (s, 1H), 6.13 (d, J = 2.4 Hz, 2H), 6.52 (dd, J = 8.6, 2.2 Hz, 2H), 7.36 (t, J = 7.4 Hz, 2H), 7.43(t, J = 7.5 Hz, 2H), 7.55–7.68 (m, 10H), 7.75 (d, J = 8.6 Hz, 2H), 7.80 (d, J = 8.0 Hz, 2H), 7.88 (s, 2H), 8.57 (d, J = 8.6 Hz, 2H).

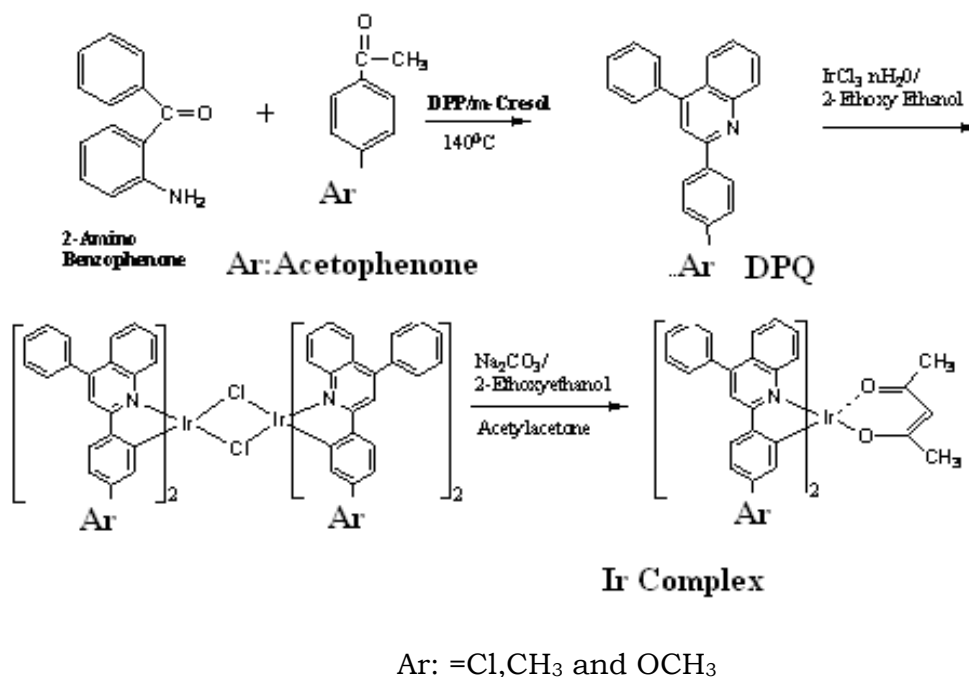


Fig.1: Scheme 1 Synthesis scheme of ligand and Iridium complex

2.2 Measurements: A SHIMADZU 8101 FTIR spectrometer was used to record (IR) spectra. ^1H -nuclear magnetic resonance (NMR) and ^{13}C -NMR spectra were recorded using 300 MHz NMR Bruker spectrometers. Thermo gravimetric analysis TGA and SDTA was performed using Mettler STARE Thermo Gravimetric Analyzer, TGA/sDTA851e. Differential scanning calorimeter (DSC) analysis was carried out under nitrogen environment using Mettler Toledo System. The XRD pattern was obtained by X-ray Panalytical diffractometer with Cu K α radiation ($\lambda=1.5418 \text{ \AA}$) operated at 40 kV and 20 mA. The optical absorption spectra of complex and ligand in basic and acidic media in different molecular concentration were obtained on an Analytik Specord-50 spectrophotometer. The photoluminescence (PL) spectra were obtained by SHIMADZU RF 5301 spectrofluorometer.

3. RESULTS AND DISCUSSION

3.1 X-Ray structural analysis:

The crystallinity of the polyquinolines was evaluated by wide-angle X-ray diffraction experiments. The X-ray diffraction analysis on powder, $\text{Ir}(\text{Cl-DPQ})_2(\text{acac})$, $\text{Ir}(\text{M-DPQ})_2(\text{acac})$ and $\text{Ir}(\text{OMe-DPQ})_2(\text{acac})$ are shown in **Fig.1,2 and 3**. From the XRD spectra it is clear that XRD spectra have many strong, sharp diffraction peaks. This indicates the crystalline character of the polymeric material. These spacing correspond to the chain distances of a well-organized molecular layer structure, which is consistent with literature reports. There are much weaker diffraction peaks indicating lower crystallinity or orientation. In addition, its higher volume fraction of insulating side chains may also contribute to its low field-effect mobility. However, too much crystallinity causes brittleness. The crystallinity parts give sharp narrow diffraction peaks and the amorphous component gives a very broad peak (halo). The ratio between these intensities can be used to calculate the amount of crystallinity in the material.

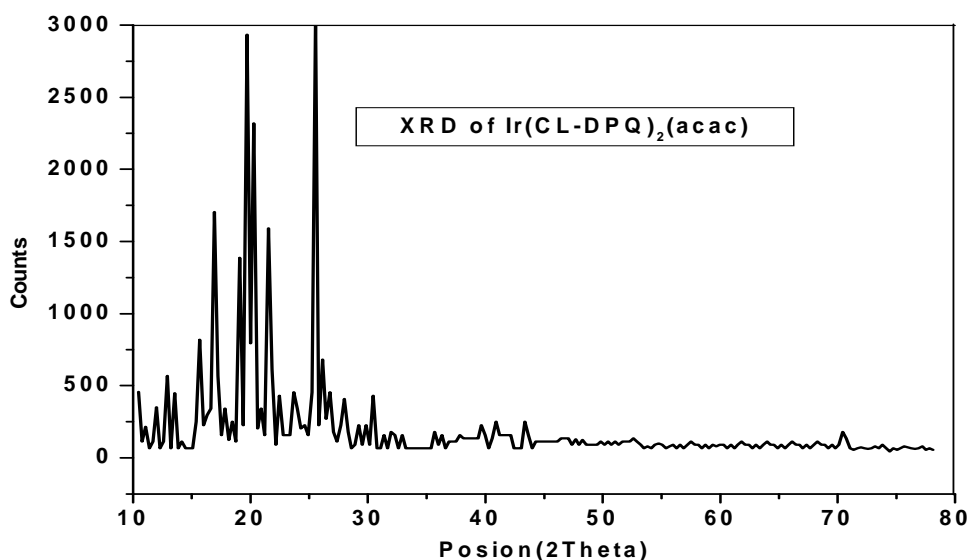


Fig. 1: XRD Pattern of $\text{Ir}(\text{Cl-DPQ})_2(\text{acac})$

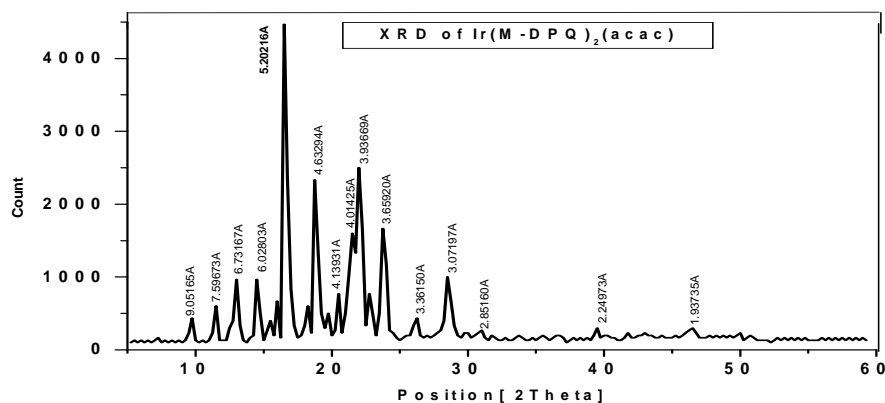


Fig.2: XRD Pattern of Ir(M-DPQ)₂(acac)

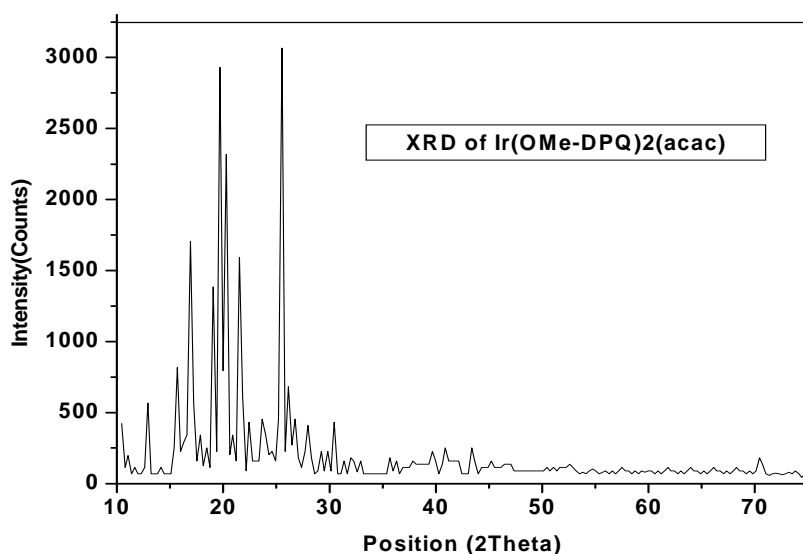


Fig. 3: XRD pattern of Ir (OMe-DPQ)₂(acac)

3.2 Thermo gravimetric Analysis:

We investigated the thermal properties of Ir(Cl-DPQ)₂(acac) and Cl-DPQ by differential scanning calorimetric (DSC). The DSC second heating scans of the polymeric compound are shown in Fig. 4 (curve (a) and Curve (b)). **Fig 4** curve (a) indicate that Cl-DPQ undergoes a glass transition at 55°C, following by crystallization at 111°C and crystalline melting point at 345 °C.. In contrast, there was no phase transition signal observed for Ir(Cl-DPQ)₂(acac) from 30 to 450 °C as shown in **Fig.4** curve (b).

We investigated the thermal properties of Ir(M-DPQ)₂(acac) and MDPQ by differential scanning calorimetry (DSC) DSC measurement are recorded on Mettler Tolloedo System at RSIC, Nagpur. The DSC second heating scans of the polymeric compound are as shown in **Fig.5**. It indicates that M-DPQ undergoes a glass transition at 43°C, following by crystallization at 103°C and crystalline melting point at 303 °C. In contrast, there was no phase transition signal observed for Ir (MDPQ)₂(acac) from 30 to 300 °C.

We investigated the thermal properties of Ir(OMe-DPQ)₂(acac) and OMe-DPQ by differential scanning calorimetry (DSC) DSC measurement are recorded on Mettler Tolloedo System at RSIC, Nagpur. The DSC second heating scans of the polymeric compound are as shown in **Fig. 5**. **Fig.3** indicate that OMe-

DPQ undergoes a glass transition at 42°C, following by crystallization at 95°C and crystalline melting point at 425 °C. In contrast, there was no phase transition signal observed for Ir (OMe-DPQ)₂(acac) from 30 to 300 °C.

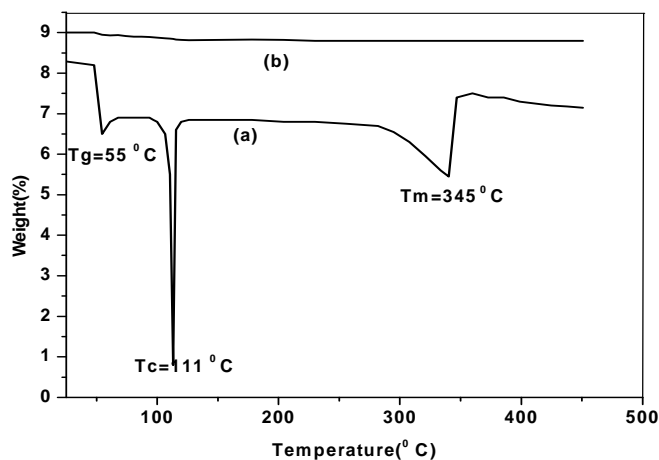


Fig.4: DSC scan of (a) Cl- DPQ.(b)Ir(Cl-DPQ)₂(acac)

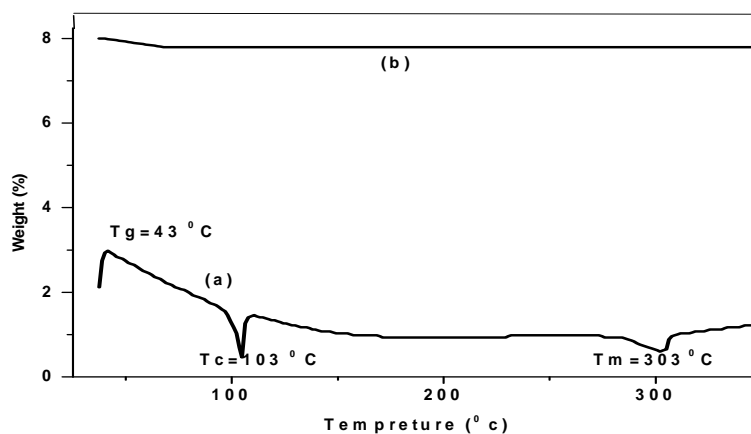


Fig. 5: DSC scan of M-DPQ and Ir (M-DPQ)₂ (acac)

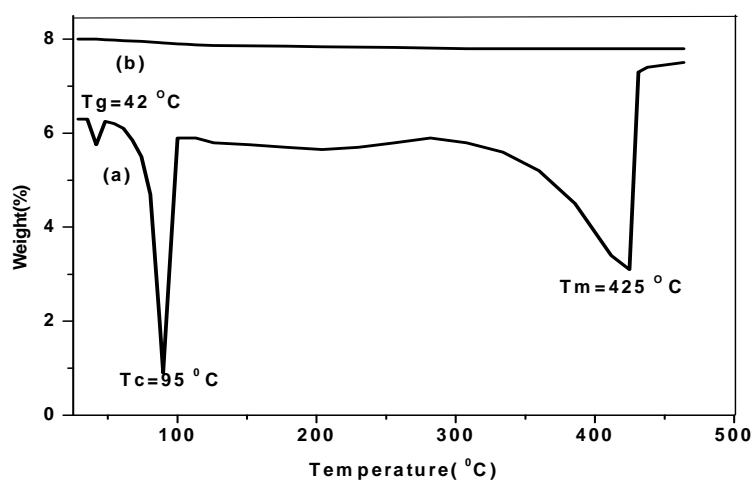


Fig. 6: DSC scans of (a)OMe – DPQ and(b) Ir(OMe-DPQ)₂(acac)

The dynamic (non-isothermal) thermo gravimetric analysis of Cl-DPQ, M-DPQ and OMe-DPQ has been carried out in air atmosphere with a heating rate $4^{\circ}\text{C} / \text{min}$. in a platinum crucible. The thermocouple used was Chromel - alumel in the temperature range $35 - 450^{\circ}\text{C}$. The TGA and SDTA curve obtained from Mettler STARe Thermo Gravimetric Analyzer, TGA/sDTA851e is shown in **Fig. 7**

Thermo gravimetric analysis plots of the Cl-DPQ, obtained under the atmosphere of nitrogen, are shown in **Fig.7**. The 10 % loss of mass for the Cl-DPQ were found to be 327°C . This result indicates that incorporation of the Cl substitution improves the thermal stability of the DPQ matrix.

TGA curve of M-DPQ (Fig.7 curve (a)) shows three steps (a) No weight loss was observed in the first step of temperature range from 38 to 68°C . i.e. there is no effect of temperature on a sample up to 68°C . (b) A small weight loss of about 1.62 % was observed in the second step of temperature ranges from 68°C to 84°C . The weight of the sample reduces to 6.735 mg. (c) The total weight loss of about 3.15 % was observed in the third step of temperature range from 84 to 97°C . In this step, the sample weight becomes 6.63 mg.

Fig.7 curve (c) shows the TGA analysis of the OMe-DPQ when it was heated to 500°C at a heating rate of $4^{\circ}\text{C}/\text{min}$ under a dry nitrogen atmosphere. The weight loss of the polymeric compound was less than 10% upon heating to 350°C , indicative of good thermal stability. The onset of thermal degradation is also shown in figure. The compound is stabled similar to DPQ. It is clearly observed that the decomposition temperature of OMe-DPQ is lower than DPQ. The decrease of the T_c of OMe-DPQ compared with DPQ could be attributed to the methoxy substituted donor group to phenyl ring. The stability of the material is adequate for the fabrication processes.

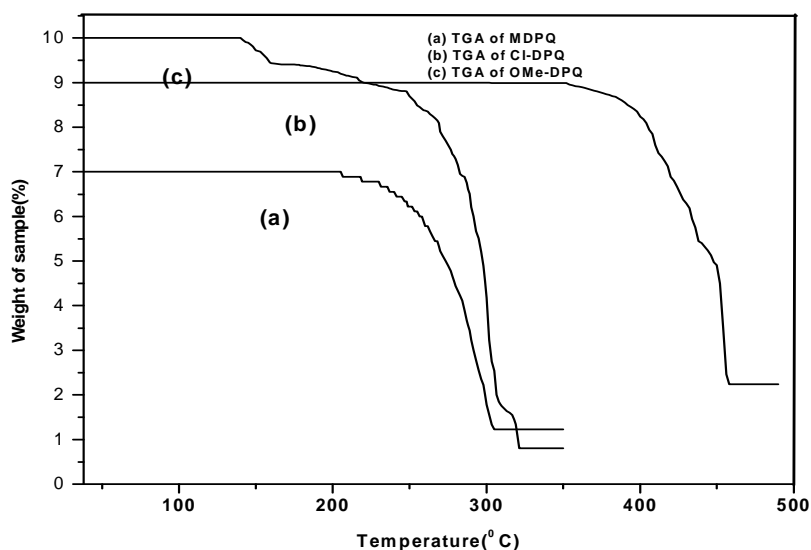


Fig.7: Thermo gravimetric analysis curve. of (a) MDPQ (b)Cl-DPQ (c)OMe-DPQ

3.3 FTIR Analysis:

The FTIR spectrum of the complex has been taken in KBr. The molecular confirmations of Iridium complexes are done by FTIR spectra. The following FTIR peaks are obtained for the complexes.

The characteristic peaks of FT-IR spectra of $\text{Ir}(\text{Cl-DPQ})_2(\text{acac})$ are 3058, 3028, 2840, 2597, 2337, 2318, 2257, 2131, 1962, 1898, 1821, 1773, 1709, 1685, 1650, 1589, 1573, 1541, 1484, 1447, 1436, 1315, 1252, 1239, 1224, 1181, 1153, 1128, 1065, 1028, 973, 925, 891, 841, 780, 756, 700, 679, 651, 590, 546 cm^{-1} .

The characteristic peaks of FT-IR spectra of $\text{Ir}(\text{M-DPQ})_2(\text{acac})$ are 3060, 3040, 2960, 2935, 2880, 2840, 1750, 1600, 1500, 1450, 1260, 1150, 790-870 cm^{-1} .

The characteristic peaks of FT-IR spectra of $\text{Ir}(\text{OMe-DPQ})_2(\text{acac})$ are 3060, 3023, 2963, 2897, 2820, 2601, 2396, 2036, 1934, 1798, 1663, 1656, 1515, 1460, 1447, 1404, 1358, 1307, 1256, 1244, 1234, 1112, 1074, 1000, 970, 957, 831, 775, 734, 679, 647, 633, 615, 588, 549, 522 cm^{-1} .

3.4 Photo physical properties:

3.4.1 Photo physical properties of ligands: The absorbance spectra of Cl-DPQ, OMe-DPQ and M-DPQ in dichloromethane solution measured at room temperature are shown in **Fig. 8**. In **Fig. 8** curve (a) shows the optical absorption spectra of Cl-DPQ in dichloromethane at room temperature. The compound Cl-DPQ shows broad absorption band ranging from 240 to 390 nm with a λ_{max} at around 260 nm and a shoulder at 330 nm respectively. The polymeric compound have broad absorption at 260 nm (4.78 eV) and 330 nm (3.76 eV) due to π - π^* transition intermolecular charge transfer in dichloromethane. The peak intensity decreases with increasing concentration of Cl-DPQ. No new absorption features were observed in the wavelength range 200 – 500 nm, suggesting that the material have no observable interaction in their electronic ground state

In **Fig. 8** (curve b), shows absorption spectra of OMe-DPQ in dichloromethane. The absorbance spectrum of the compound is characterized by a strong absorption peak centered at 272 nm with a weak shoulder at 332 nm. This peak should be due to the diphenyl ring in OMe-DPQ.

The spectra are identical to that of 2, 4-DPQ as a result of the weak inductive effect of the methoxy group. The maximum peak observed for asymmetric OMe-DPQ exhibits a significant red shift relative to that of 2, 4-DPQ ($\lambda_{\text{max}} = 254 \text{ nm}$), suggesting strong π - π^* conjugation. This observation is consistent with a recent study on the distinct photo physical properties observed in 2, 4-DPQ. When compared the optical absorption of OMe-DPQ is bathochromically shifted by 10-15 nm, indicating that the methoxy substituent plays a role in determining the gap between the highest occupied molecular orbital (HOMO) and the lowest unoccupied molecular orbital (LUMO).

In **Fig. 8** (curve c), shows absorption spectra of M-DPQ in dichloromethane. The absorbance spectrum of the compound is characterized by a strong absorption peak centered at 268 nm with a weak shoulder at 336 nm. This peak should be due to the diphenyl ring in M-DPQ.

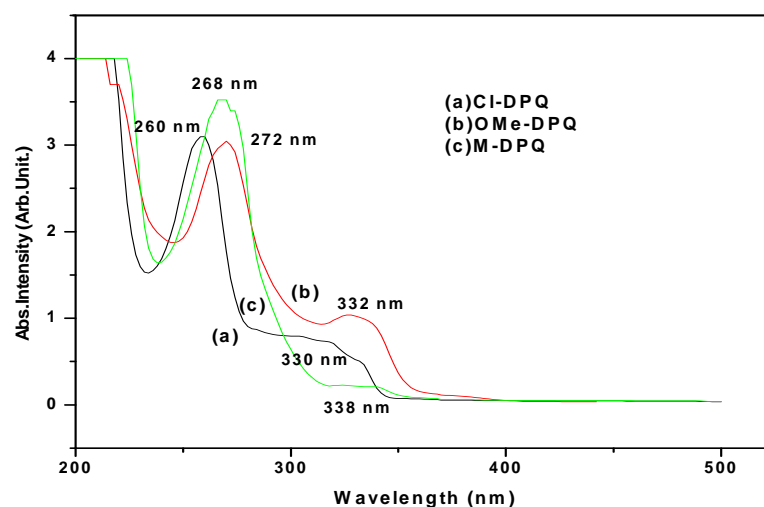


Fig.8: Absorption spectra for (a)Cl-DPQ(b) OMe-DPQ and (c)M-DPQ in dichloromethane solution.

The PL emission spectra Cl-DPQ in dichloromethane solution are shown in **Fig. 9** Curve (a) When the Cl-DPQ in dichloromethane solution is excited at 395 nm, it emits intense blue light of wavelength 450 nm.. The red shift of 14 nm is found due Cl group substitution as compared to 2, 4-DPQ. The FWHM value of PL spectrum is 49 nm.

The dilute-solution (diff. molar conc.) excitation and photoluminescence (PL) spectra of OMe-DPQ in DCM are studied. The PL spectra of the polymeric compound OMe-DPQ in dichloromethane with excitation wavelength 368 nm at concentration 10^{-6} M are shown in Fig.9 curve (b). When the excitation wavelength was 368 nm, it was observed that the PL intensity is higher in concentrated spectrum than dilute spectrum. The main peaks are appeared at 430 nm (curve b) in dichloromethane .

The photoluminescence (PL) spectra of 10^{-6} M solutions of M-DPQ complex in DCM at room temperature are shown in **Fig. 9** (Curve c). A M-DPQ ligand shows photoluminescence peak at 510 nm in DCM solution when excited at 370 nm.

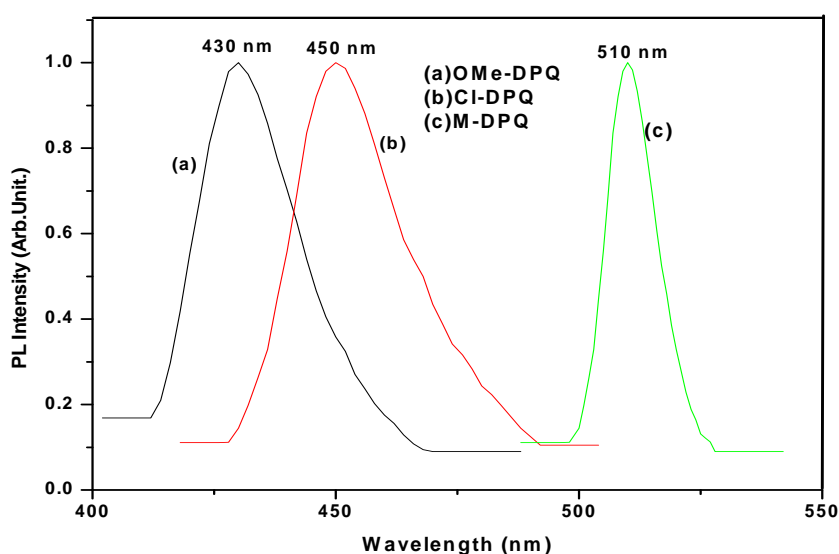


Fig.9: PL spectra for (a) OMe-DPQ (b) Cl-DPQ and (c) M-DPQ in dichloromethane solution.

3.4.2 Photo physical properties of iridium complex: The absorption and emission spectra measured for $\text{Ir}(\text{Cl-DPQ})_2(\text{acac})$, $\text{Ir}(\text{OMe-DPQ})_2(\text{acac})$ and $\text{Ir}(\text{M-DPQ})_2(\text{acac})$ in THF solution at room temperature. are shown in **Fig 10**. We assign the strong absorption bands in the UV region to the spin-allowed $^1\pi-\pi^*$ transition of the cyclometalated quinoline ligands. Relative to the absorption band of $\text{Ir}(\text{DPQ})_2(\text{acac})$, we observe a significant bathochromic shift for $\text{Ir}(\text{Cl-DPQ})_2(\text{acac})$, $\text{Ir}(\text{OMe-DPQ})_2(\text{acac})$ and $\text{Ir}(\text{M-DPQ})_2(\text{acac})$, which results from the ligand. The next lowest energy absorption, with peak wavelengths in the region 440–460 nm, can be ascribed to a typical spin-allowed metal-to-ligand charge transfer ($^1\text{MLCT}$) transition; we believe the weak bands at long wavelengths are associated with both spin-orbit coupling enhanced $^3\pi-\pi^*$ and $^3\text{MLCT}$ transitions. It is noteworthy that the formally spin forbidden $^3\text{MLCT}$ gains intensity by mixing with the higher-lying $^1\text{MLCT}$ transition through the strong spin-orbit coupling on Ir, which results in an intensity that is comparable with the allowed $^1\text{MLCT}$. We observed highly intense photoluminescence (PL) for $\text{Ir}(\text{Cl-DPQ})_2(\text{acac})$, $\text{Ir}(\text{OMe-DPQ})_2(\text{acac})$ and $\text{Ir}(\text{M-DPQ})_2(\text{acac})$ in THF with values of λ_{max} located at 620 nm, 610 nm and 650 nm respectively. The broad, structure less spectral features lead us to conclude that the phosphorescence originates primarily from the $^3\text{MLCT}$ state. It has been demonstrated that the HOMO and LUMO of cyclometalated complexes of the $\text{Ir}(\text{ppy})_3$ type are located mainly at the Ir-phenyl center and the electron-accepting heterocyclic portion of

the ligands, respectively With respect to $\text{Ir}(\text{PQ})_2(\text{acac})$, which has an emission maximum at 599 nm, the 4-phenyl substituent in the DPQ ligand leads to a bathochromic shift of ca. 16 nm in the emission peak wavelength, which can be rationalized qualitatively by considering the decrease in the LUMO energy level that results from an increase in the p-conjugation length of the quinoline moiety that is induced by the 4-phenyl group. In comparison with $\text{Ir}(\text{DPQ})_2(\text{acac})$, which incorporates a cyclometalated phenyl group, $\text{Ir}(\text{Cl-DPQ})_2(\text{acac})$, which bears [2- (-4 Chloro phenyl)- 4phenyl quinoline (Cl-DPQ)] a Chloro phenyl group, reveals an additional 5 nm red shift in the emission maxima that we attribute to the extended p conjugation raising the HOMO energy level. These observations are in accordance with the results of the electrochemical analysis.

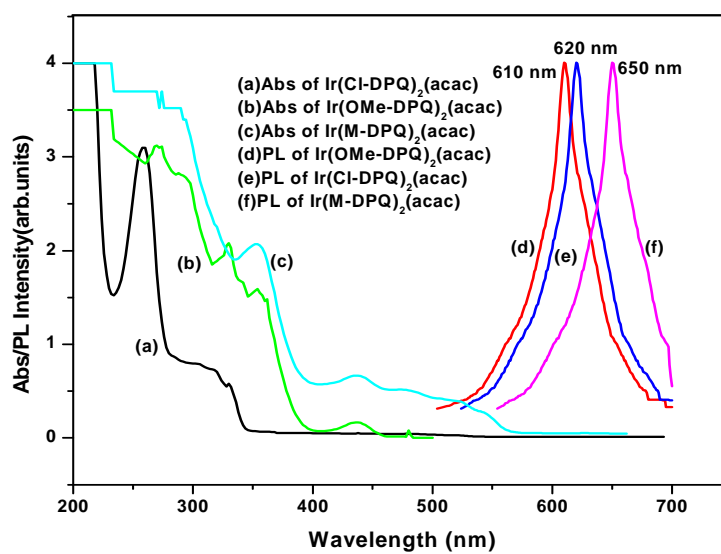


Fig.10: Absorption and PL emission spectra for Iridium in THF solution.

4. CONCLUSION

In conclusion, we have successfully synthesized iridium complexes containing substituted 2,4 diphenyl quinoline derivatives as ligands. These complexes exhibit very high HOMO levels compared to pyridine based iridium complexes. In view of the variation of the 2,4 diphenyl quinoline ligands that can be synthesized from the method shown in Scheme 1, these complexes are strongly phosphorescent at ambient condition and emit red color. Further investigation on the effects on luminescent properties depending on tuning the substituent into various positions of the 2,4 diphenyl quinoline ligand is currently in progress. Efforts towards the development of red color complexes using different substituents are currently underway.

REFERENCES

1. M.A. Baldo, D.F. O'Brien, Y. You, A. Shoustikov, S. Sibley, M.E. Thompson, S.R. Forrest, *Nature*, 1998, 395, 151.
2. M.A. Baldo, S. Lamansky, P.E. Burrows, M.E. Thompson, *Appl. Phys. Lett.*, 1999, 75, 4.
3. S. Lamansky, P. Djurovich, D. Murphy, F. Abdel-Razzaq, H. Lee, C. Adachi, P.E. Burrows, S.R. Forrest, M.E. Thompson, *Inorg. Chem.*, 2001, **40**, 1704.
4. M.E. Thompson, P.E. Burrows, S.R. Forrest, *Solid State Mater. Sci.*, 1999, **4**, 369.
5. A. Köhler, J.S. Wilson, R.H. Friend, *Adv. Mater.* 2002, **14**, 701.

6. A.J. Lees, *Chem. Rev.*, 1987, **87**, 711.
7. I.M. Dixon, J.P. Collin, J.P. Sauvage, L. Flamigni, S. Encinas, F. Barigelletti, *Chem. Soc. Rev.*, 2000, **29**, 385.
8. V.W.W. Yam, K.K.W. Lo, *Chem. Soc. Rev.*, 1999, **28**, 323.
9. D.S. Tyson, J. Bialecki, *F.N. Chem. Commun.*, 2000, **4**, 2355.
10. V.W.W. Yam, S.W.-K. Choi, K.K. Cheung, *Organometallics*, 1996, **15**, 1734.
11. V.W.W. Yam, K.L. Yu, K.M.C. Wong, K.K. Cheung, *Organometallics*, 2001, **20**, 721.
12. Q.Z. Yang, L.Z. Wu, Z.X. Wu, L.P. Zhang, C.H. Tung, *Synth. Met.*, 1998, **94**, 245.
13. Y. Ma, C.M. Che, H.Y. Chao, X. Zhou, W.H. Chan, J. Shen, *Adv. Mater.*, 1999, **11**, 852.
14. S. Lamansky, P. Djurovich, D. Murphy, F. Abdel-Razzaq, H.E. Lee, C. Adachi, P.E. Burrows, S.R. Forrest, M.E. Thompson, *J. Am. Chem. Soc.*, 2001, **123**, 4304.
15. Ramchandra Pode and Jang Hyuk Kwon Chapter IV of book "Organic Light Emitting Diode – Material, Process and Devices" 2011, 101-146.
16. A. Tsuboyama, H. Iwawaki, M. Furugori, T. Mukaide, J. Kamatani, S. Igawa, T. Moriyama, S. Miura, T. Takiguchi, S. Okada, M. Hoshino, & K. Ueno *J. Am. Chem. Soc.* 2003, **125**, 12971.
17. H. K. Dahule, S. J. Dhoble and Ramchandra Pode *J. Search and Research* 2011, **III**, 75.
18. B. X. Mi, P. F. Wang, Z. Q. Gao, C. S. Lee, S. T. Lee, H. L. Hong, X. M. Chen, M.S. Wong, P. F. Xia, K. W. Cheah, C. H. Chen, and W. Huang, *Adv. Mater.* 2009, **21**, 339.
19. T.C. Lee, C.F. Chang, Y.C. Chiu, Y. Chi, T.Y. Chan, Y.M. Cheng, C.H. Lai, P.T. Chou, G.H. Lee, C.H. Chien, C.F. Shu, & J. Leonhardt, *An Asian Journal*, 2009, **4**, 742.
20. W. Lu, B.X. Mi, M.C.W. Chan, Z. Hui, N. Zhu, S.T. Lee, C.M. Che, *Chem. Commun.* 2002, 206.
21. B.W. D'Andrade, J. Brooks, V. Adamovich, M.E. Thompson, S.R. Forrest, *Adv. Mater.* 2002, **14**, 1032.
22. J. Brooks, Y. Babayan, S. Lamansky, P.I. Djurovich, I. Tsyba, R. Bau, M.E. *Inorg. Chem.*, 2002, **41**, 3055.
23. Tsujimoto, S. Yagi, H. Asuka, Y. Inui, S. Ikawa, T. Maeda, H. Nakazumi, & Y. Sakurai, *J. of Organometallic Chemistry*, 2010, **695**, 1972.
24. Thejo Kalyani, S.J. Dhoble, R.B. Pode, *Adv. Mat. Lett.*, 2011, **21**, 65.
25. H.K. Dahule, S.J. Dhoble, J.S. Ahn, and R.B. Pode, *J. of Phy. & Chem. of Solids*, 2011, **72**, 1524.
26. R. Pode, K.H. Kim, J.H. Kwon, S.J. Lee, I.A. Shin, & S.H. Jin, *J. Phys. D: Appl. Phys.*, 2010, **43**: 025101-1 – 025101-5.
27. S.B. Raut, S.J. Dhoble and R.G. Atram, *Synthetic Metals* 2011, **161**, 391.

28. Y.Wang, X.Deng, Y.Liu, M.Ni, M.Liu, H.Tan, X.Li, W.Zhu, Y.Cao, *Tetrahedraon*, 2011,**67**,2118.
29. M.A.Tehfe, J.Lalevee, S.Telitel, J.Sun,J.Zhao, B.Graff, F.M.Savary, J.P.Fouassier, *Polymer*, 2012,**53**,2803.
30. J.H.Jou, M.C.Tang, P.C..Chen, Y.S.Wang,S.M.Shen, B.R.Chen, C.H.Lin, W.B.Wang, S.H.Chen, C.T.Chen, F.Y.Tsai, C.W.Wang,C.C.Chen, C.C.Wang, *Organic Electronic*, 2012,**13**, 1349.
31. E.A. Fehnel, *J. Org. Chem.*, 1966, **31**, 2899.
32. M.Nonoyama, *Bull. Chem. Soc. Jpn.* 1974, **47**, 767.

***Corresponding Author: S.J.Dhoble**, Department of Physics, RTM Nagpur University,Nagpur
440033, India